MOLECULAR PHYSICS, 1993, VOL. 79, No. 5, 1087–1101

The temperature dependence of fast vibrational energy transfer processes in methyl fluoride

By HENRY O. EVERITT
US Army Research Office, PO Box 12211, Research Triangle Park, North Carolina, USA

and FRANK C. DE LUCIA
Department of Physics, Ohio State University, 174 W 18th Avenue, Columbus, Ohio 43210, USA

(*Received 1 December 1992; accepted 8 December 1992*)

The temperature dependencies of two fast vibrational energy transfer processes in methyl fluoride (CH_3F) have been measured between 120 K and 400 K by means of time-resolved millimetre/submillimetre-infrared double resonance spectroscopy. The first of these processes, a resonant vibrational swapping process between the ground vibrational state and the $\nu_3 = 1$ (ν_3) vibrational state, effectively transfers population between states of A and E symmetry. A rapid increase in cross section with decreasing temperature was observed for this process, a result in excellent quantitative agreement with semi-classical theory of near resonant vibrational collisions. The second process, which transfers population between the ν_3 and $\nu_6 = 1$ (ν_6) vibrational states, was found experimentally to have a much weaker temperature dependence. From this result and from additional experimental observations of symmetry type-sensitive energy transfer into ν_6, the energy transfer between ν_3 and ν_6 was demonstrated to result from a 'direct' vibrational energy transfer rather than from an 'indirect' vibrational swap process.

1. Introduction

We have previously reported a series of studies designed to investigate collisionally induced rotational and fast vibrational transitions in the polyatomic molecule CH_3F [1–6]. A goal of this work has been the development of a numerical model which describes the wide variety of observable phenomena in terms of only a few physically meaningful molecular parameters. We have in large part accomplished this goal.

In this paper we pursue a deeper understanding of the nature of collisional processes by observing and measuring vibrational energy transfer mechanisms as a function of temperature. The rates of these processes will be described by fundamental molecular parameters such as dipole moment and vibrational oscillator strength. The temperature variation of the rates will be introduced by proper consideration of well defined temperature dependent molecular quantities such as partition functions and molecular velocities.

We specifically consider the temperature dependence of the mechanisms which are responsible for two fast vibrational transitions in CH_3F: the $v_3 = 1$ (ν_3) vibrational swapping process, responsible for effectively moving population between the

A and E symmetry species of CH_3F, and the energy transfer process connecting the ν_3 vibrational state to that with $v_6 = 1$ (ν_6). Even though these two vibrational state-changing processes are among the fastest in CH_3F, it will be shown that they operate via fundamentally different mechanisms. The new, temperature-dependent data also provide stringent tests of vibrational energy transfer theories because significant changes in cross-section can occur in the region between 120 K and 400 K; changes which such theories must predict with no adjustable parameters.

2. Summary of previous work

The characterization of rotational energy transfer in polyatomic molecules can be complex because of the large number of energetically available states and the myriad collisional rates which couple them. One of the most important findings of our previous work is that hierarchical models may be developed which can be expanded to simultaneously account for all observable data, or which can be collapsed to make possible simplified studies of subsets of the more general problem. These hierarchical models are based on the empirical fact that large numbers of rotational states are in thermal equilibrium with one another for substantial periods of time during the evolution of the systems; therefore, each group of states can be considered collectively as a pool during these periods. While part of this hierarchy is based on the relative speed of the processes, molecular symmetries and selection rules play an important role [7].

For the studies described in this paper, the model shown in figure 1 is appropriate. The ν_3 vibrational states lies approximately $1050\,cm^{-1}$ above the ground state, with ν_6 lying approximately $135\,cm^{-1}$ higher. As a result of symmetries associated with nuclear spin statistics, the individual rotational energy levels within a particular vibrational state are designated as having either A or E symmetry [8]. On the time scale of these experiments (< 1 ms), collision-induced interconversion between the two symmetry species is very rare because the nuclei themselves are only coupled weakly to the outside world. Therefore, two pools exist for each vibrational state, one for each symmetry type. The population in these pools is the sum of the original population in these rotational states plus the pump-induced, rotationally thermal population changes.

The population in states near the pump-connected states is most strongly perturbed. The population in these few states is comprised of the 'thermal population' (the state's fraction of the thermally distributed 'pool' molecules) and state-specific 'non-thermal population' (the excess/deficit state-specific population caused by the pump and collisional processes) [3–6]. Because the pump creates excess non-thermal population in ν_3 by creating deficit non-thermal population in the ground vibrational state, the sum of all non-thermal population is zero at all times. Therefore, microscopic reversibility must be maintained in the model in a seemingly counter-intuitive manner: although population flow between thermal pools or between non-thermal states is two-way, population flow between thermal pools and non-thermal states is one-way.

The millimetre/submillimetre wave-infrared (mm/submm-ir) double resonance experimental technique used to study rotational and vibrational energy transfer has been discussed previously [5, 6, 9, 10]. The mm/submm radiation is generated from a phase-locked klystron operating at 35 GHz coupled to a frequency multiplier. The harmonic of the klystron fundamental coincident with the centre frequency of

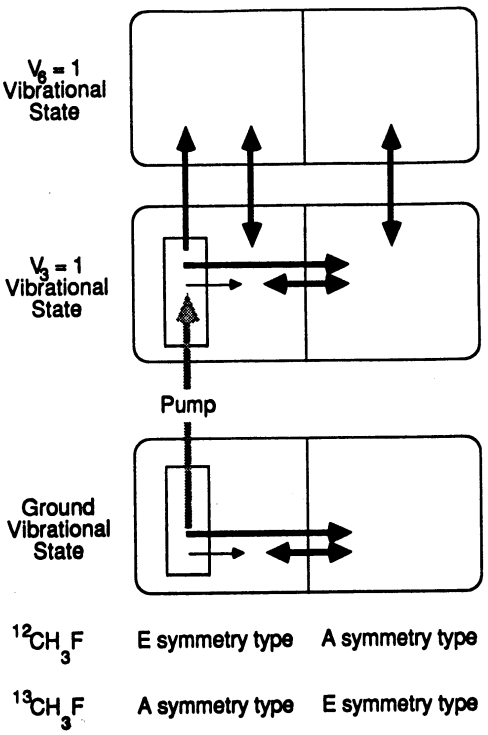

Figure 1. Numerical simulation used in this study to model energy transfer processes in $^{12}CH_3F$ and $^{13}CH_3F$. Shown schematically are the A and E symmetry pools in the ground, ν_3, and ν_6 vibrational states (large rounded boxes), the collection of non-thermal states (vertical rectangles), the CO_2 laser pump (light vertical arrow), and the collisional energy transfer processes (other arrows). The V-swap process is represented by the bold horizontal arrows and the $\nu_3 \rightarrow \nu_6$ process is represented by the bold vertical arrows. The $\Delta K = 3n$ process is represented by the narrow horizontal arrow, and the vibrational relaxation processes are not shown.

the rotational transition of interest is propagated through a 1 cm radius, 1·5 m long copper diagnostic cell and detected by an InSb detector cooled to about 1·5 K. After preamplification, the time-dependent signal is acquired by a fast CAMAC-based DSP Technology, Inc. signal averager followed by a Macintosh II computer. The tunability of the mm/submm source is sufficient for the observation of rotational transitions of frequency up to at least 600 GHz throughout ν_3 and ν_6.

The temperature of the cell could be cooled to any temperature between 77 K and 300 K by flowing liquid nitrogen through a cooling jacket surrounding the cell or could be heated to about 400 K using external resistance heating tapes. Thermostatic control and uniform cooling/heating maintained the temperature of the cell to within 5 K. Because of the temperature gradient between the diagnostic cell and the capacitance manometer, a thermal transpiration correction was used to convert the displayed pressure to reflect the actual gas pressure in the cell [11]. The experiments were performed at a variety of sample gas pressures, and the uncertainty of the pressure was less than 1 mTorr.

Co-propagated through the cell is a pump CO_2 laser beam whose $\sim 1\,\mu s$ Q-switched pulses create non-equilibrium population distributions in a specific rotational state of the probed excited vibrational state. In $^{13}CH_3F$, the frequency of a 9P32 CO_2 laser is coincident with an absorption in the A symmetry species due to the

transition between the $J = 4$, $K = 3$ level of the ground state and $J = 5$, $K = 3$ level of ν_3. Similarly, the 9P20 line of the CO_2 laser pumps population from the $J = 12$, $K = 2$ level of the E symmetry species of the ground vibrational state of $^{12}CH_3F$ to the $J = 12$, $K = 2$ level of ν_3. In our experiments, the pump pulses deposited population into the upper state in a time short compared with the subsequent collisional relaxation. The collisional processes among the subject molecules spread population away from the pumped rotational state into other rotational states, including the monitored states. The changing population in these states yields a measurable, time-evolving rotational absorption strength.

The model of figure 1 outlines the energy transfer simulation used to extract the rate constants from the data for the collisionally induced transitions. Time-dependent energy transfer is simulated by allowing population to flow from a given state/pool to another state/pool. The rate at which the population flows is either known from earlier work or extracted from the data using the model. In the latter case, the results of the simulation were compared with the time-resolved experimental data, and the unknown energy transfer rate constants were refined via the technique of nonlinear least squares fitting. Measured rate constants were converted into cross sections using $\sigma = 0{\cdot}0505k\,(Tm)^{1/2}$, where σ is the cross-section (Å^2), k is the measured rate constant (msec^{-1} mTorr^{-1}), T is the temperature (K), and m is the molecular mass (amu).

In our earliest work [1] we observed that continuously pumping a rotational level in one of the ν_3 symmetry species of CH_3F produced essentially equal steady state populations in states of *both* symmetry species. On the surface, this is somewhat surprising because 'direct' transitions between states of E and A symmetry are forbidden to high order. Stated another way,

$$CH_3F\,(A, n\nu_i) + CH_3F \not\leftrightarrow CH_3F\,(E, n\nu_i) + CH_3F, \tag{1}$$

for any molecule of symmetry type A or E in the vibrational state $n\nu_i$. However, the vibrationally resonant swapping, or V-swap, process can take place. By this process, a molecule in the excited vibrational state collides with a molecule in the ground vibrational state and exchanges vibrational quanta. These 'indirect' V-swap collisions come in several forms,

$$CH_3F\,(A, \nu_3) + CH_3F'\,(E, \nu_0) \leftrightarrow CH_3F\,(A, \nu_0) + CH_3F'\,(E, \nu_3), \tag{2a}$$

$$CH_3F\,(A, \nu_3) + CH_3F'\,(A, \nu_0) \leftrightarrow CH_3F\,(A, \nu_0) + CH_3F'\,(A, \nu_3), \tag{2b}$$

$$CH_3F\,(E, \nu_3) + CH_3F'\,(E, \nu_0) \leftrightarrow CH_3F\,(E, \nu_0) + CH_3F'\,(E, \nu_3), \tag{2c}$$

the most interesting of which (2*a*) effectively transfers population between the symmetry species in the excited (and ground) state. Since this process is vibrationally resonant and the transition moment is large for the $\nu_3 \leftrightarrow$ ground state transition, ν_3 V-swap in CH_3F can have a large cross-section. Because the ground state population is essentially thermal, because the selection rules associated with the process only allow small changes in rotational quantum number, and because most of the collision partners for the excited state CH_3F are part of this ground state pool, the thermal distribution of the ground state pool is transferred essentially unaltered to the excited state. In other words, V-swap populates ν_3 rotational states with a Boltzmann distribution to both symmetry species. The two symmetry species equilibrate because V-swap is much faster than competing vibrational relaxation. That

V-swap maintains a thermal distribution is the principal justification for use of the simplified model of figure 1 for this study.

The work described in this paper also addresses an interesting question about the collisionally induced transfer of population from ν_3 to ν_6; specifically, is this an indirect near-resonant V-swap or a direct vibrational energy transfer process? Consider an observation that illustrates the difference between the two mechanisms. If the process is direct,

$$CH_3F\,(A,\,\nu_3) + CH_3F\,(A/E,\,\nu_0) + \Delta E \leftrightarrow CH_3F\,(A,\,\nu_6) + CH_3F\,(A/E,\,\nu_0), \quad (3a)$$

or

$$CH_3F\,(E,\,\nu_3) + CH_3F\,(A/E,\,\nu_0) + \Delta E \leftrightarrow CH_3F\,(E,\,\nu_6) + CH_3F\,(A/E,\,\nu_0), \quad (3b)$$

it must obey the nuclear spin-induced selection rule, transferring population from ν_3 to ν_6 without altering symmetry type. Therefore, the pump-induced early time non-equilibrium between A and E symmetry species in ν_3 would be manifested by an observable early time non-equilibrium between those species in ν_6. Early time is defined as the time scale during which the ν_3 V-swap processes has not equilibrated A and E in ν_3.

Alternatively, if the $\nu_3 \rightarrow \nu_6$ process is an indirect V-swapping mechanism:

$$CH_3F\,(A,\,\nu_3) + CH_3F'\,(E,\,\nu_0) + \Delta E \leftrightarrow CH_3F\,(A,\,\nu_0) + CH_3F'\,(E,\,\nu_6), \quad (4a)$$

$$CH_3F\,(E,\,\nu_3) + CH_3F'\,(A,\,\nu_0) + \Delta E \leftrightarrow CH_3F\,(E,\,\nu_0) + CH_3F'\,(A,\,\nu_6), \quad (4b)$$

$$CH_3F\,(A,\,\nu_3) + CH_3F'\,(A,\,\nu_0) + \Delta E \leftrightarrow CH_3F\,(A,\,\nu_0) + CH_3F'\,(A,\,\nu_6), \quad (4c)$$

$$CH_3F\,(E,\,\nu_3) + CH_3F'\,(E,\,\nu_0) + \Delta E \leftrightarrow CH_3F\,(E,\,\nu_0) + CH_3F'\,(E,\,\nu_6), \quad (4d)$$

the essentially thermal population of the ground state will be deposited in ν_6, resulting in the same population in both symmetry species at all times. In addition to this test, theory suggests that these two mechanisms have different temperature dependences that can be compared with the new experimental observations as an additional check of the type of process.

3. Vibrational swapping collisions

In the near-resonant vibrational swapping processes illustrated by equation (2), simultaneous rotational and vibrational transitions are induced in the colliding molecules. The size of the net energy defect $\Delta E = \Delta E_1 + \Delta E_2$ plays an important role in determining the probability of a collision-induced transition, where ΔE_i is the total rotational (ΔE_{ri}) and vibrational (ΔE_{vi}) energy change of molecule i. The calculation of the vibrational contribution to this energy defect is straightforward, but the calculation of the rotational contribution and the subsequent thermal averaging over the collision partners is more complex. Because of the limitation placed on rotational quantum number change by the order of the multipole moments which contribute to the collision [7], each ΔE_{ri} is typically $\ll kT$. The restriction is especially severe for dipole–dipole interactions ($\Delta J = 0, \pm 1$, $\Delta K = 0$). Similarly, the size of the allowed vibrational change is determined by the order of the derivative of the interacting moment, with collisions mediated by dipole first derivative 'interactions' limited to $\Delta V = \pm 1$. A process may be considered near-resonant if $\Delta E_v = \Delta E_{v1} + \Delta E_{v2} \ll kT$.

Because such a small amount of net energy is transferred during near-resonant collisions, interactions can primarily take place in the weak interaction regime where long-range attractive intermolecular forces are dominant. Consequently, the behaviour of near-resonant collisions may be described in a manner similar to the description of rotational energy transfer collisions. Indeed, near-resonant vibrational swaps may be viewed as the dipole–dipole interaction of vibrational energy transfer. However, unlike rotational collisions, the cross-section for near-resonant transitions is related to the derivative of multipole moment rather than the moment itself. Thus, near-resonant collisions have smaller cross sections than pure rotational collisions, but in comparison with other vibrational processes near-resonant collisions may be extremely fast.

A theory describing near-resonant vibrational 'swaps', based on Anderson–Tsao–Curnutte (ATC) theory [12] and developed by Sharma and Brau (SB) [13], has been used to predict cross sections for near-resonant collisions. Originally developed to predict the cross-section for the N_2–CO_2 energy transfer responsible for the CO_2 laser, this theory may also be applied to the V-swap process in CH_3F–CH_3F collisions.

As in ATC theory, molecules are assumed to travel in classical straight-line trajectories, whereas rotational and vibrational motions are treated quantum mechanically. For the case of CH_3F, the derivative of the dipole moment is so large that, as a first approximation, all other derivatives of multipole moments may be ignored. Using first-order perturbation theory with a potential containing only this highest-order non-zero moment for each colliding molecule, the probability for an induced transition for a specific collision velocity, impact parameter, and net energy defect may be calculated.

In the ATC-like derivation, first-order perturbation theory shows that the probability of a state-changing collision may be factored into time-independent transition matrix elements and a time-dependent term which contains the energy mismatch. Specifically

$$p_{i\to f} = \left|\frac{1}{\hbar}\int e^{i\omega_T t} < \Psi'_0(f)|V(t)|\Psi'_0(i) > \mathrm{d}t\right|^2$$

$$= \left|\sum_m M_{l,m} I_{l,m}(\omega_T)\right|^2 \tag{5}$$

where $V(t)$ is the standard multipolar potential for axially symmetric molecules written in terms of spherical harmonics with respect to molecule-fixed coordinates and containing time-dependent intermolecular separations R [7, 14]. $\omega_T = (\Delta E_1 + \Delta E_2)/\hbar$ is the energy mismatch of the collision, and $l = l_1 + l_2$ is the sum of the orders of the moments involved in the collision. For dipole–dipole interactions, $l = 1 + 1 = 2$, and the time-independent rovibrational dipolar transition matrix elements for the colliding molecules summed over m are

$$M_2 = \langle J'_1, K_1, V'_1|\mu_1|J_1, K_1, V_1\rangle\langle J'_2, K_2, V'_2|\mu_2|J_2, K_2, V_2\rangle. \tag{6}$$

The term including the energy mismatch components of the collision,

$$I_{2,m} = -\frac{1}{\hbar}\sqrt{\frac{8\pi}{3}}\int \frac{Y_{2,m}(\hat{R})}{R^3} e^{i\omega_T t}\,\mathrm{d}t, \tag{7}$$

explicitly contains time dependence of the dipole–dipole interaction in the energy mismatch exponent and implicitly contains time dependence in R.

There are several important points to be made about these equations. Contained in M_2 are rotational transition matrix elements which determine the branching ratios for each rotational transition. Note that changes in rotational state, governed by dipole–dipole selection rules, and changes in vibrational stae ($\Delta V = \pm 1$ for dipole-derivative mediated interactions) are allowed in this approximation. The transition probability is directly proportional to the square of the dipole-derivative matrix element of each colliding molecule. For homomolecular V-swap collisions, the vibrational portions of the matrix elements are identical so the transition probability is proportional to the fourth power of the dipole-derivative vibrational transition matrix element.

Much of the work in evaluating the transition probability comes from evaluating $I_{2,m}$. Sharma and Brau reduce this factor by using a polynomial expansion on $\omega_T b/v$, where b is the impact parameter of the collision. Averaging this probability over a Maxwell–Boltzmann distribution of velocities v and summing over m yields

$$P_{i\to f}(b, \omega_T, T) = \frac{8m^*}{3\hbar^2 b^4 (kT)} (M_2)^2 \Gamma(b, \omega_T, T), \tag{8}$$

where m^* is the reduced molecular mass. The resonance term Γ calculates the propensity of a swap based upon net energy defect (including vibrational energy defect, if any) of the collision just as in ATC theory. $\Gamma(b, \omega_T, T)$ strongly discriminates against large energy mismatch collisions. Therefore, the cross section for vibrationally resonant V-swaps is dominated by collisions whose net rotational energy defect is close to zero with respect to kT. A combination of small impact parameters, large dipole derivative matrix elements, and small vibrational defects must exist for a near-resonant vibrational state-changing process to occur.

This equation also reveals a strong dependence upon impact parameter b. To proceed with the evaluation of this transition probability between two molecules in specified rovibrational states, $P_{i\to f}$ must be averaged over the impact parameter. Since integration over the impact parameter is quite involved, Sharma and Brau approximate this integration by evaluating Γ for $b = 0$ and for the gas kinetic collision diameter $b = d$. Then they parabolically interpolate between these values to estimate Γ in the range $0 \leq b \leq d$, and assume $P \sim b^{-4}$ for $b > d$. The resulting equation,

$$\langle P \rangle = \tfrac{1}{2} P_{i\to f}(0, \omega_T, T) + \tfrac{3}{2} P_{i\to f}(d, \omega_T, T), \tag{9}$$

gives the transition probability of a specific V-swap collision involving two (dipolar) molecules in specific states.

From this the partial and total cross sections for the near-resonant process may be calculated by averaging over the rotational distribution of population in the collision partners and in both molecules, respectively. For example, the cross section for the V-swap process between the ν_3 state and the ground state of CH_3F at 300 K is calculated to be 27 Å^2. This is comparable in size to the CH_3F gas kinetic collision cross section of 44 Å^2, suggesting that V-swap in ν_3 should be an important process. Indeed, this process has been observed at room temperature in ν_3, and the calculated cross-section is in good agreement with our experimentally measured value of $21{\cdot}0 \pm 2{\cdot}1$ Å^2 (see table 1). This result is gratifying considering the uncertainties in the values of d ($3{\cdot}75 \pm \sim 0{\cdot}10$ Å) [14] and the derivative of the dipole moment for the $\nu_3 \to \nu_0$ transition ($0{\cdot}2756 \pm 0{\cdot}0085$ Debye) [15], especially since each of these parameters is raised to a high power in the calculation.

Table 1. Temperature dependent cross-sections of fast vibrational energy transfer in CH_3F.

Process	Temperature/K	$^{12}CH_3F$ $\sigma/Å^2$	$^{13}CH_3F$ $\sigma/Å^2$
ν_3 V-swap	120	50·6(10)	54·1(1)
	150	43·4(20)	52·3(15)
	200	36·4(21)	36·2(10)
	250	22·8(9)	30·2(16)
	300	18·9(15)	21·0(21)
	350	15·6(10)	16·8(28)
	400	13·4(35)	13·6(19)
$\nu_3 \rightarrow \nu_6$	300		2·65(11)
	350		2·63(25)
	400		2·34(7)

Next, consider the temperature dependence of the V-swap cross section σ_{VS} in the context of equation (8). Both the resonance term Γ and the leading term have temperature dependencies. The resonance condition is relaxed in Γ with rising temperature because of the increasing collision velocities. However, the rotational partition function grows with rising temperature, decreasing the probability of molecular collisions with small rotational defects. Detailed calculations for CH_3F show that after all of the appropriate averages over the thermal populations have been made, these two effects closely balance one another over the temperature range of this study. Thus, the resonance contribution to the cross section for these collisions is temperature insensitive, and the temperature dependence of σ_{VS} is found to be approximately $1/T$.

These calculations assume a rotationally thermal distribution of population within the vibrational states. However, when the laser pulse transfers population into an excited vibrational state, a large fraction of the population of the excited vibrational state will initially reside in the pumped rotational state. Since the V-swap process operates via near-resonant collisions, the fact that so much population resides in one rotational state of a molecule can narrow the number of collision partner states with which a molecule may have a near-resonant collision. As an extreme test of this, if *all* the population of the $^{13}CH_3F$ ν_3 vibrational state resides in one rotational state ($J = 5$, $K = 5$), then the ν_3 V-swap cross section at 300 K is calculated to be about 30 Å^2, in contrast with the calculated value of 27 Å^2 for a Boltzmann-distributed ν_3. Moreover, in this extreme case the distribution of population initially placed into ν_3 by the V-swap process differs markedly from the Boltzmann distribution obtained if ν_3 is distributed in a Boltzmann manner. Although in principle these differences impact the validity of the simple model of figure 1, other faster processes effectively cause equilibrium within a symmetry species before too much of the swapping process has occurred [5].

Figure 2 displays the time response of the $J = 4$–5, $K = 3$ transition of the ν_3 A pool in $^{12}CH_3F$ at 120 K following the transfer of population into the ν_3 E pool by the Q-switched CO_2 laser pump. Figure 2 also displays the $J = 2$–3, $K = 2$ transition of the ν_3 E pool in $^{13}CH_3F$ at 120 K following the pump-induced transfer of population into the ν_3 A pool. Time responses similar to figure 2 have been observed over a wide range of ν_3 A states in $^{12}CH_3F$ ($J = 2$–3 through $J = 9$–10, $K = 0$ and 3) and a wide range of ν_3 E states in $^{13}CH_3F$ ($J = 1$–2 through $J = 10$–11, $K = 1$, 2, and 4),

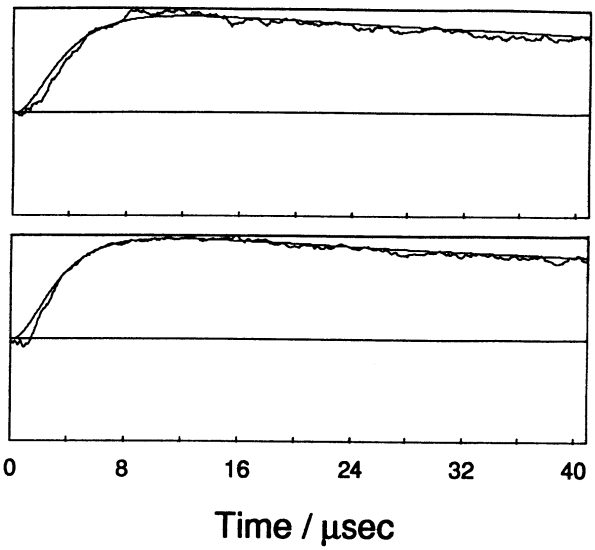

Figure 2. The upper trace is the time response of the $J = 4$–5, $K = 3$ (A-type) transition in the ν_3 state of $^{12}CH_3F$ at 120 K and 25 mTorr following the pumping of an E-type state. The lower trace is the time response of the $J = 2$–3, $K = 2$ (E-type) transition in the ν_3 state of $^{13}CH_3F$ at 120 K and 25 mTorr following the pumping of an A-type state. Fits from the simulation overlay the data.

many at a number of temperatures. (V-swap was also observed and measured in both isotopes in states of the same symmetry type as the pumped state. These data have been summarized recently [16, 17] and are to be elaborated in a future article.) The increase in population following the pump pulse results from the action of the V-swap process, while the subsequent decay of population toward equilibrium is mainly due to well-understood vibrational relaxation resulting from molecular collisions with the cell wall. Because of a near coincidence (−157 MHz) of the 9P32 pump transition with the $J = 4$, $K = 2$, $\nu_0 \rightarrow J = 5$, $K = 2$, ν_3 transition in $^{13}CH_3F$, those states with $K = 2$ experienced weak, early-time non-equilibrium. This non-equilibrium thermalized quickly enough that it did not affect the measurement of the V-swap rate constant.

A numerical simulation based on the simple model of figure 1 was used to find the rate constant of the V-swap process at each temperature. The rate constant was measured using a nonlinear least squares technique to fit the predictions of the simulation over the observed time responses as shown in figure 2. Fits were performed for a number of thermal transpiration-corrected pressures (typically 10 to 50 mTorr and 120 to 400 K) for both isotopes of CH_3F. For example, the room temperature rate constant for the ν_3 V-swap process in $^{13}CH_3F$ was found to be $4{\cdot}1 \pm 0{\cdot}4\,\text{msec}^{-1}\,\text{mTorr}^{-1}$, corresponding to about two gas kinetic collisions. The rate constants are converted to cross sections (see table 1) and plotted as a function of temperature in figure 3. These results show no systematic variation with isotope or 'pumped' symmetry type. The solid line in figure 3, given by $\sigma_{VS} = 8000/T\,\text{Å}^2$, represents the results of theoretical calculations based on the theory of Sharma and Brau using the molecular parameters presented earlier. As can be seen, the agreement between the predicted and observed temperature dependence of the cross section is very good with no parameters adjusted. (Alternatively, a fit of the data in figure 3 yields a temperature dependence for the ν_3 V-swap cross section of $\sigma_{VS} =$

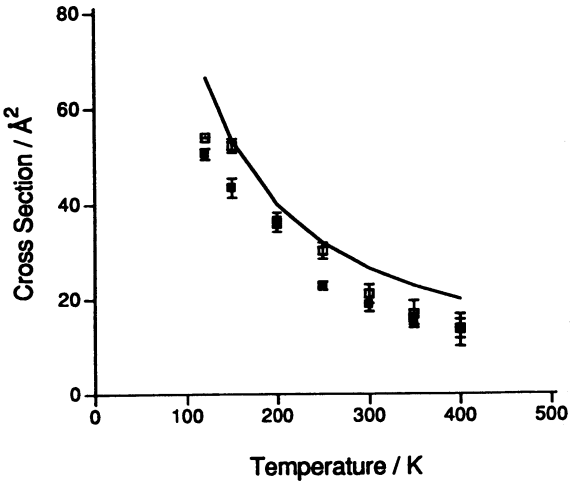

Figure 3. A comparison of the observed $^{12}CH_3F$ (filled boxes), observed $^{13}CH_3F$ (open boxes) and predicted (solid line) V-swap cross sections as a function of temperature.

$6475/T$ Å^2.) The excellent agreement between theory and experiment is in part due to the fact that the dipole derivative is so large that other moments do not contribute significantly and may be ignored in this calculation. These other moments may be more important in molecules or states with weaker dipole derivatives and should be considered in those calculations.

Preses and Flynn [18] have measured the cross section of a process closely related to the pure ν_3 V-swap process discussed above. In their experiments, ν_3 of $^{12}CH_3F$ was excited by a pump laser, and the transfer of this excitation to ν_3 of $^{13}CH_3F$ was observed via cw CO_2 laser probe. Although pure V-swap and near resonant isotopic transfer V-swap processes differ by a small vibrational energy defect, SB theory predicts that the effect of this defect is relatively small and that the two cross sections should be similar. However, Preses and Flynn measured the rate constant of the isotopic transfer V-swap process to be $1{\cdot}5\,\text{msec}^{-1}\,\text{mTorr}^{-1}$, about a quarter the value of the rate constant of the pure ν_3 V-swap process at the same temperature (about 235 K).

Moreover, Sheorey and Flynn [19] measured a 12 Å^2 cross section for the process whereby two molecules in ν_3 collide, placing one in $2\nu_3$ and one in the ground state. This room temperature cross section, which is slightly less than twice the cross section of the isotopic transfer process, is consistent with expectations of the vibrational state-dependent scaling based upon the increasing size of the vibrational matrix element with increasing vibrational excitation. It would appear that the differences in these measurements, all of which are experimentally and conceptually straightforward, provide a basis for a more detailed analysis of the roles of energy defects, vibrational anharmonicities, and temperature in these processes.

Recently Matsuo and Schwendeman [20] and Shin, Song and Schwendeman [21] have also observed the V-swap process operating in the both $^{13}CH_3F$ and $^{12}CH_3F$ using infrared–infrared double resonance. They confirmed the rotationally thermal nature of the process; however, the focus of their study was the measurement of collisionally induced changes in the velocity of the pumped molecules. There were no such velocity effects witnessed in the states connected to the pumped state through V-swap. In other words, these states had the expected doppler-broadened Gaussian

lineshape typical of a transition made up of molecules with a thermal distribution of the translational degrees of freedom. Therefore, the V-swap process fills ν_3 in a thermal manner, both rotationally and translationally, as anticipated from the thermal distribution of the ground state.

4. Collisional energy transfer between ν_3 and ν_6

The V-swap process of equation (4) is an example of an 'indirect' vibrational state-changing process which takes place via energetically near-resonant swaps of vibrational quanta between molecules resulting from interactions with the long-range attractive portion of the intermolecular potential. By contrast, most vibrational state-changing processes occur through 'direct', energetically non-resonant changes in a given molecules's vibrational state (equation (3)) and may only be caused by hard collisions involving the strongly repulsive portion of the intermolecular potential. The process transferring population between ν_3 and ν_6 involves an intermediate energy gap (about $135\,\mathrm{cm}^{-1}$) in which either or both might be important. Our goal was to find out which of these two mechanisms is dominant.

Let us first consider the prediction of theory. As we have seen, the ATC-like theory of Sharma and Brau has succeeded in describing near-resonant vibrational energy transfer. However, the semi-classical theoretical descriptions of direct, non-resonant collisions are less successful. The reasons for this are manifold, related primarily to the inability of the multipole expansion to properly describe close, hard collisions. Nevertheless, it is instructive to estimate the relative sizes of the cross-sections of these two mechanisms.

The indirect vibrational energy transfer theory of Sharma and Brau involves the dipole derivatives of both colliding molecules as well as the energy defect. Because the dipole derivative for the $\nu_0 \rightarrow \nu_6$ transition is very small, this factor, when combined with the relatively large vibrational energy defect of $135\,\mathrm{cm}^{-1}$, results in a calculated $\nu_3 \rightarrow \nu_6$ rate for equation (4) orders of magnitude slower than the gas kinetic collision rate. Thus, if the calculation is valid in this regime, ν_6 is likely populated by other, faster processes.

The direct vibrational energy transfer theory developed by Schwartz, Slawsky, and Herzfeld (SSH), often referred to as the 'breathing sphere' theory illustrates the dependence of direct transfer on vibrational state-dependent parameters [22–24]. The probability (per gas kinetic collision) of vibrational energy transfer (equation (3)) for a given relative collision velocity v is

$$p_{i\rightarrow f}(v) = \left[\frac{1}{\hbar}\langle \Psi' | V | \Psi \rangle\right]^2, \tag{10}$$

where V is the interaction potential. If it is assumed that the zero-order wavefunctions are separable in the N normal vibrational coordinates Q_k and in the intermolecular separation R, then V may be approximated as a product of functions in these coordinates given by

$$V = V_T(R)V_1(Q_1)\cdots V_N(Q_N). \tag{11}$$

This factorization may only be made if it is further assumed that the molecules do not rotate during the collision. Although this is certainly not true over the entire course of the approach and retreat of the molecules, this assumption is justified during the extremely short time the molecules are close enough to cause a

vibrational exchange. Because rotation is ignored, SSH theory only treats collisions which convert vibrational energy defect into translational energy, so-called V → V and V → T collisions.

The matrix elements for the $V_k(Q_k)$ are easily evaluated by assuming the vibrations of mode k may be described by harmonic oscillator wavefunctions. The squares of the matrix elements are

$$[V_k]^2 = 1,$$

$$[V_k]^2 = \alpha^2 \langle A_k^2 \rangle \left[\frac{\hbar}{2\omega_k}(V+1)\right] = 496 \frac{\langle A_k^2 \rangle}{E_k}(V+1), \tag{12}$$

for the V → V and V → V + 1 intramode transitions, respectively. The term $\langle A_k^2 \rangle$ (amu^{-1}) is the average displacement of the vibrating atoms per unit change in the normal coordinate Q_k, $\alpha \approx 5{\cdot}6\,\text{Å}^{-1}$ is an approximately molecule independent repulsion factor obtained by matching an exponential to the repulsive portion of the intermolecular potential [25]. ω_k and E_k are the characteristic vibrational frequency and energy (cm^{-1}) of the kth mode, respectively. The matrix element for intermode transitions is the product of two intramode matrix elements. For example, the matrix elements for the $\nu_3 \rightarrow \nu_6$ process are $[V_3]^2[V_6]^2$.

Like the dipole derivative matrix elements in near-resonant vibrational collision theory, these breathing sphere amplitude factors $\langle A_k^2 \rangle$ play a crucial role in determining the cross section of a non-resonant vibrational state-changing collision. The values of these amplitude factors have been calculated by Stretton [25] for the lowest excited vibrational states of CH_3F. As an example of the application of these amplitude factors, Stretton's [25] calculation of the room temperature V → T deexcitation probability from one of these states to the ground state reveals a surprising result. The de-excitation probability for CH_3F is predicted to be about twice as large for ν_6 as it is for ν_3, even though ν_3 is lower in energy. The reason for this is directly attributable to the much larger amplitude factor for ν_6. The sum of the V → T processes, $(\nu_3 \rightarrow \nu_0) + (\nu_6 \rightarrow \nu_0)$, is approximately 52 000 gas kinetic collisions, about five times slower than actually observed. For the $\nu_3 \rightarrow \nu_6$ process of interest here, SSH theory predicts that the cross section for the direct, non-resonant vibrational state-changing process is 44 gas kinetic collisions. Since this is much larger than the calculated indirect vibrational swapping cross section for $\nu_3 \rightarrow \nu_6$, theoretical calculations suggest that direct energy transfer, not vibrational swapping, is the dominant mechanism responsible for $\nu_3 \rightarrow \nu_6$.

We have measured the 300 K rate constant for the $\nu_3 \rightarrow \nu_6$ process in $^{13}CH_3F$ to be $0{\cdot}512 \pm 0{\cdot}021\,\text{msec}^{-1}\,\text{mTorr}^{-1}$, or about 17 gas kinetic collisions. Typical time responses are shown in figure 4, and the experimentally measured temperature dependence of this cross section is shown in figure 5. No ν_6 time response signals could be detected for temperatures much lower than room temperature, so there are no measured cross sections there. For temperatures above 300 K there was only a weak decrease in cross section with increasing temperature. The 300 K result concurs with the earlier 300 K $^{12}CH_3F$ rate constant measurements of Sheorey and Flynn [26] of $0{\cdot}631 \pm 0{\cdot}034\,\text{msec}^{-1}\,\text{mTorr}^{-1}$, and is in fairly good agreement with the 300 K SSH calculation. However, the agreement between experiment and theory is probably coincidental because the calculations predict an increasing cross section with increasing temperature.

The double resonance time-resolved experimental technique can be used to

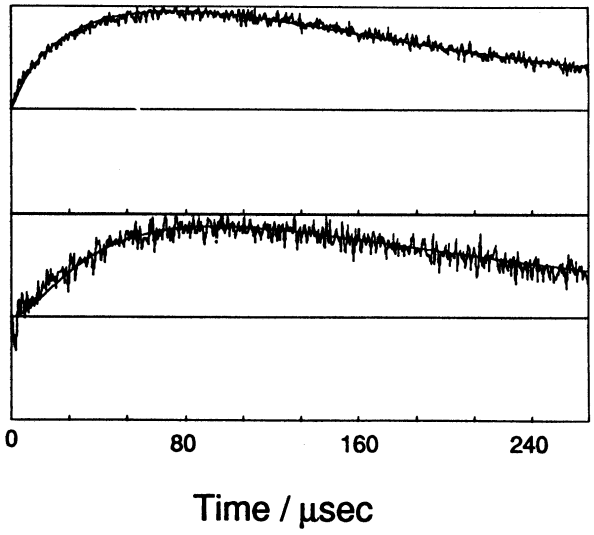

Figure 4. The upper time response is for the $J = 4$–5, $K = 2$, $l = -1$ (A-type) transition in ν_6 of $^{13}CH_3F$, and the lower time response is for the $J = 4$–5, $K = 2$, $l = +1$ (E-type) transition. (State $J = 5$, $K = 3$ (A-type) of ν_3 is pumped.) The difference at early time is due to the direct transfer of population from ν_3 just after the pump-induced non-equilibrium. The pressure is 40 mTorr asnd the temperature is 300 K. The early negative spike on the lower trace is a lasing artifact.

monitor the population transfer from ν_3 into either the ν_6 A or the ν_6 E partitions individually. Utilizing this state-specificity, we were able to demonstrate conclusively that the dominant mechanism responsible for $\nu_3 \rightarrow \nu_6$ transfer is the direct process represented by equation (3). Since the ν_3 V-swap rate is significantly faster than the $\nu_3 \rightarrow \nu_6$ rate, the responses of A and E states in ν_6 will be similar. However, the apparatus is sensitive enough to detect early-time, collisionally induced non-equilibrium in ν_6 at very early times while ν_6 still exhibits strong non-equilibrium between A and E. Thus, if the dominant process connecting ν_3 and ν_6 is a direct process, the experiment will be able to observe the non-equilibrium in ν_6.

The $^{13}CH_3F$ ν_6 time response data and simulated time response shown in figure 4

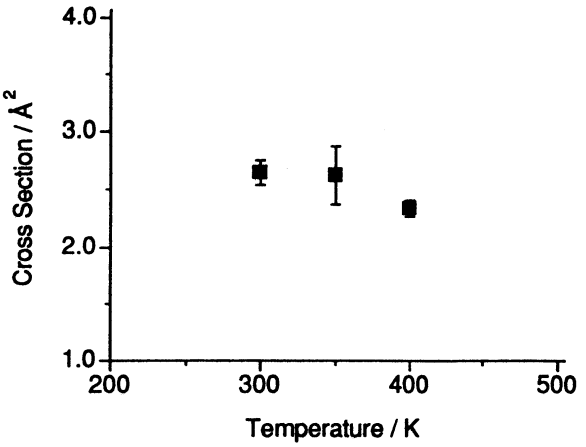

Figure 5. Measured cross-sections for vibrational energy transfer from ν_3 to ν_6 as a function of temperature.

confirms that the transfer is dominated by a direct process. Since an A state of ν_3 is pumped, the A states in ν_6 should rise faster at early times than the E states. Although the observed time responses of A and E are similar, the difference at early time is discernible. Because the cross section of the ν_3 V-swap process decreases with increasing temperature while the cross section of the $\nu_3 \rightarrow \nu_6$ process remains fairly constant, the early-time differences should grow larger with increasing temperature. The 350 and 400 K time response data (not shown here) experimentally verify this.

The population growth in the ν_6 E symmetry species proceeds through a two-step process: a ν_3 V-swap from the A pool to the E pool followed by a direct $\mathrm{E}\,\nu_3 \rightarrow \mathrm{E}\,\nu_6$ process. The parallel process $\mathrm{A}\,\nu_3 \rightarrow \mathrm{A}\,\nu_6$ followed by a $\nu_6\,\mathrm{A} \rightarrow \mathrm{E}$ V-swap should be exceedingly slow because V-swap in ν_6 is predicted to much slower than in ν_3.

Finally, it is important to note that the only fitted rate constant in the simulated time response overlaying figure 4 is the rate constant for $\nu_3 \rightarrow \nu_6$ direct vibrational transfer (equation (3)). The non-equilibrium observed in the data between the ν_6 A and E time-response data is *predicted* by the model based entirely upon its simulation of the time-dependent non-equilibrium in ν_3 and its use of the previously measured ν_3 V-swap rate. The enhanced early-time non-equilibrium of ν_6 A and E states at high temperatures is similarly predicted by the simulation; indeed, all ν_6 time responses at all temperatures were fitted successfully with one one adjustable parameter: the $\nu_3 \rightarrow \nu_6$ rate constant.

5. Summary

In this paper we have reported the results of millimetre/submillimetre wave-infrared double resonance measurements of the cross sections for two fast vibrational processes in CH_3F at various temperatures. The vibrationally resonant V-swap process was observed operating between ν_3 and the ground state of both $^{12}CH_3F$ and $^{13}CH_3F$. The cross section of this process, which decreased with increasing temperature as $1/T$, was observed to be insensitive to isotope and symmetry type. On the other hand, the non-resonant process connecting the vibrational states ν_3 and ν_6 was observed to have a smaller, temperature insensitive cross-section. It was also clearly demonstrated that energy transfer proceeds directly between these two vibrational states and therefore is not an indirect mechanism like V-swap.

A goal of this work was to provide stringent tests of theoretical explanations for vibrational state-changing processes by requiring the theories to describe the results without resorting to additional empirical parameters. The semiclassical theory of Sharma and Brau successfully predicted the cross sections for the V-swap mechanism in the ν_3 vibrational state with essentially no adjustable parmeters. This was especially impressive because of the approximate 350% variation of this cross section over the observed 120 K to 400 K temperature range.

Because of the absence of a detailed theory for the collisional process which directly transfers population from ν_3 to ν_6. SSH theory has been used to estimate the propensity for such direct processes in terms of more fundamental molecular parameters. The fact that the $\nu_3 \rightarrow \nu_6$ process is a direct energy transfer process results from the fact that the amplitude vibration factor of the ν_6 mode is large whereas the derivative of the dipole moment for the $\nu_6 \rightarrow \nu_0$ transition is quite small. Direct vibrational state-changing collisions like the $\nu_3 \rightarrow \nu_6$ process involve harder, more energetic collisions; consequently, theories describing them require

both a better understanding of the interaction potential and a consideration of many more collision channels. These new data should provide additional opportunities for tests of such theories.

The authors would like to thank D. Skatrud for helpful comments during the preparation of this manuscript. The authors would also like to acknowledge the support of the Army Research Office and the National Science Foundation.

References

[1] Matteson, W. H. and De Lucia, F. C., 1983, *IEEE J. quant. Electron*, **QE-19,** 1284.
[2] Matteson, W. H. and De Lucia, F. C., 1985, *J. opt. Soc. Am.* B, **2,** 336.
[3] McCormick, R. I., De Lucia, F. C. and Skatrud, D. D., 1987, *IEEE J. quant. Electron*, **QE-23,** 2060.
[4] McCormick, R. I., Everitt, H. O., De Lucia, F. C. and Skatrud, D. D., 1987, *IEEE J. quant. Electron.*, **QE-23,** 2069.
[5] Everitt, H. O. and De Lucia, F. C., 1989, *J. chem. Phys.*, **90,** 3520.
[6] Everitt, H. O. and De Lucia, F. C., 1990, *J. chem. Phys.*, **92,** 6480.
[7] Oka, T., 1973, *Adv. at. Mol. Phys.*, **9,** 127.
[8] Gordy, W. and Cook, R. L., 1984, *Microwave Molecular Spectra* (Wiley Interscience).
[9] King, W. C. and Gordy, W., 1953, *Phys. Rev.*, **90,** 3139.
[10] Everitt, H. O., Skatrud, D. D. and De Lucia, F. C., 1986, *Appl. Phys. Lett.*, **49,** 995.
[11] Poulter, K. F., Rodgers, M. J., Nash, P. J., Thompson, T. J. and Perkin, M. P., 1983, *Vacuum*, **33,** 311.
[12] Tsao, C. J. and Curnutte, B., 1962, *J. quant. Spectrosc. radiat. Transfer*, **2,** 41.
[13] Sharma, R. D. and Brau, C. A., 1969, *J. chem. Phys.*, **50,** 924.
[14] Hirchfelder, J. O., Curtis, C. F. and Bird, R. B., 1964, *Molecular Theory of Gases and Liquids* (Wiley).
[15] Kondo, S., Koga, Y. and Nakanaga, T., 1986, *J. phys. Chem.*, **90,** 1519.
[16] Everitt, H. O., 1990, PhD dissertation, Duke University (unpublished).
[17] Goyette, T. M., McCormick, R. I., De Lucia, F. C. and Everitt, H. O., 1992, *J. molec. Spectrosc.*, **153,** 324.
[18] Preses, J. M. and Flynn, F. W., 1977, *J. chem. Phys.*, **66,** 3112.
[19] Sheorey, R. S. and Flynn, G., 1980, *J. chem. Phys.*, **72,** 1175.
[20] Matsuo, Y. and Schwendeman, R. H., 1989, *J. chem. Phys.*, **91,** 3966.
[21] Shin, U., Song, Q. and Schwendeman, R. H., 1991, *J. chem. Phys.*, **95,** 3964.
[22] Schwartz, R. N., Slawsky, Z. I. and Herzfeld, K. F., 1952, *J. chem. Phys.*, **20,** 1591.
[23] Schwartz, R. N. and Herzfeld, K. F., 1954, *J. chem. Phys.*, **22,** 767.
[24] Tanczos, F. I., 1956, *J. chem. Phys.*, **25,** 439.
[25] Stretton, J. L., 1965, *Trans. Faraday Soc.*, **61,** 1053.
[26] Sheorey, R. S. and Flynn, G., 1980, *J. chem. Phys.*, **72,** 1175.